Limnol. Oceanogr., 53(1), 2008, 148–159

Tidal marshes as a source of optically and chemically distinctive colored dissolved organic matter in the Chesapeake Bay

Maria Tzortziou[1]
University of Maryland, Earth System Science Interdisciplinary Center, College Park, Maryland 20742;
Smithsonian Environmental Research Center, Edgewater, Maryland 21037

Patrick J. Neale
Smithsonian Environmental Research Center, Edgewater, Maryland 21037

Christopher L. Osburn
U.S. Naval Research Laboratory, Washington, District of Columbia 20375

J. Patrick Megonigal
Smithsonian Environmental Research Center, Edgewater, Maryland 21037

Nagamitsu Maie and Rudolf Jaffé
Southeast Environmental Research Center, Florida International University, Miami, Florida 33199

Abstract

The role of tidal marshes as a source of dissolved organic carbon (DOC) and colored dissolved organic matter (CDOM) for adjacent estuarine waters was studied in the Rhode River subestuary of the Chesapeake Bay. Water in a tidal creek draining brackish, high-elevation marshes was sampled every hour during several semidiurnal tidal cycles in order to examine the tidal exchange of dissolved organic matter (DOM). Water leaving the marsh during ebbing tide was consistently enriched in DOC compared to water entering the marsh during flooding tide. There was a net DOC export from the marsh to the estuary during seasons of both low and high marsh plant biomass. Optical analysis demonstrated that, in addition to contributing to the carbon budgets, the marsh had a strong influence on the estuary's CDOM dynamics. Marsh-exported CDOM had optical properties that were consistently and markedly different from those of CDOM in the adjacent estuary. Specifically, marsh CDOM had: (1) considerably stronger absorption, (2) larger DOC-specific absorption, (3) lower exponential spectral slope, (4) larger fluorescence signal, (5) lower fluorescence per unit absorbance, and (6) higher fluorescence at wavelengths >400 nm. These optical characteristics are indicative of relatively complex, high-molecular-weight, aromatic-rich DOM, and this was confirmed by results of molecular-weight-distribution analysis. Our findings illustrate the importance of tidal marshes as sources of optically and chemically distinctive dissolved organic compounds, and their influence on CDOM dynamics, DOC budgets, and, thus, photochemical and biogeochemical processes, in adjacent estuarine ecosystems.

[1] Corresponding author (martz@code613-3.gsfc.nasa.gov; tel: 301-614-6048; fax: 301-614-5903).

Acknowledgments

We thank Jesse Phillips-Kress, James Duls, Sam Benson, and Sharyn Hedrick for assistance in the field, and Donald Weller for assistance in preparing the map of station locations. We also thank Associate Editor Elizabeth Canuel and two anonymous reviewers for their constructive comments.

Support for this work was provided by the Smithsonian Institution Fellowship program and National Aeronautics and Space Administration–Goddard Space Flight Center. Field work on Chesapeake Bay was funded in part by United States Environmental Protection Agency, Coastal Intensive Site Network (CISNet) Program through grant R826943, and Science to Achieve Results (STAR) Program through grant RD83087801, and by the Smithsonian Environmental Sciences Program.

This is Southeast Environmental Research Center contribution 359.

Dissolved organic matter (DOM) plays a key role in a broad range of processes and climate-related biogeochemical cycles in aquatic ecosystems, affecting carbon dynamics, nutrient availability, phytoplankton activity, microbial growth, and ecosystem productivity. The light-absorbing component of the DOM pool, known as colored dissolved organic matter (CDOM), is a major determinant of the amount and quality of the underwater light field. This, in turn, controls exposure of aquatic organisms to biologically damaging ultraviolet (UV) radiation and affects aquatic photochemistry and ocean color (e.g., Bricaud et al. 1981; Vodacek et al. 1997; Pienitz and Vincent 2000).

Estuarine and coastal-margin ecosystems are hot spots of DOM cycling because of intense physical and biological activity. In these systems, DOM composition and dissolved organic carbon (DOC) quality are controlled by the relative

strength of many different DOM sources as well as the complex interactions of physical, photochemical, and microbial processes that affect DOM distribution, transformation, and degradation (e.g., Sholkovitz 1976; Kieber et al. 1990; Moran and Zepp 1997). Terrestrially derived organic matter, introduced to aquatic ecosystems mainly through river and wetland discharge, is the major source of DOM in nearshore waters. Aquatic-derived inputs from living phytoplankton, microbial degradation of detritus, and zooplankton grazing also contribute to the DOM pool in the coastal zone (e.g., Carder et al. 1989; Hedges 1992; Maie et al. 2006). Despite large inputs, terrigenous DOM contributes only a small part of the total DOM pool in the open ocean (e.g., Hedges 1992; Opsahl and Benner 1997), suggesting rapid cycling and high remineralization rates, through both photochemical and biological processes, within estuarine and coastal marine environments.

Since Teal's (1962) studies on energy flow through a salt-marsh ecosystem, there has been great interest in the contribution of tidal marshes to the carbon budget of coastal zones. Although there is no consensus on the magnitude and direction of marsh–estuary net (particulate and dissolved) organic fluxes, most studies suggest that salt marshes export DOC to the adjacent estuarine ecosystem (e.g., Nixon 1980 and references therein; Jordan and Correll 1991; Peterson et al. 1994). Measurements of the tidal exchange of nutrients by Jordan et al. (1983) showed that, on a yearly basis, the brackish tidal marshes in the Rhode River subestuary of the Chesapeake Bay act as transformers of particulate to dissolved matter, exporting DOC. Moran et al. (1991) used lignin phenols as vascular plant biomarkers to show that dissolved material derived from *Spartina alterniflora* plants in salt marshes can be the source of up to 36% of nearshore DOC, and up to 20% of inner-shelf DOC, along the Georgia coast. Based on measurements of lignin phenol concentrations, Moran and Hodson (1994) estimated that 11–75% of the dissolved humic substances on the southeastern U.S. continental shelf originate in vascular plant-dominated environments, with about equal contributions from coastal salt marshes and river export. Using a stable-isotope tracer approach, Peterson et al. (1994) showed that *Spartina patens*–dominated salt marshes were a major source of DOC to Fourleague Bay in the Gulf of Mexico.

These studies, among others, show that tidal marshes may act as important local sources of bulk DOC to coastal waters. However, little is known about the optical quality, composition, and processing of this material within marsh–estuarine ecosystems. Because the origin and history of CDOM determine its chemical structure and optical signature, CDOM optical properties have been successfully used for tracing the sources and transformation pathways of dissolved material in nearshore waters (e.g., McKnight et al. 2001; Belzile et al. 2002; Jaffé et al. 2004). Previous studies have shown that CDOM absorption spectral shape and molar absorptivity can provide information about the aromatic content and average molecular weight of dissolved material (e.g., Chin et al. 1994; Blough and Green 1995). The ratio of CDOM fluorescence to absorption has been proposed as an indicator of DOM molecular weight (e.g., Stewart and Wetzel 1980; Belzile and Guo 2006). Fluorescence peaks at long wavelengths (i.e., >400 nm) have been associated with the presence of terrigenous, plant- or soil-derived CDOM (e.g., Belzile et al. 2002). Yet, studies on the optical signature of marsh-derived CDOM are scarce (Miller et al. 2002; Lu et al. 2003; Alberts et al. 2004). As a result, we know little about the effects of marsh DOM inputs on light availability and photochemistry in adjacent estuarine waters, or on the linkages between the optical properties of this material and its quality, degradability, and environmental dynamics.

The Chesapeake Bay Estuary, along the western Atlantic coast, is the largest estuary in the United States and, historically, one of the most productive in the world. Brackish and freshwater tidal marsh systems cover a large area (about 700 km^2) along the western and eastern shores and play a potentially important role in the complex biogeochemical processes, optics, and exchanges taking place in these highly dynamic coastal margins. In this study, we measured DOC concentration and CDOM optical properties over several semidiurnal tidal cycles in brackish marshes of the Rhode River subestuary along the western shore of the Chesapeake Bay. Measurements were performed during seasons of both low and high marsh plant biomass. Our main objective was to assess whether the marshes are a source of optically and compositionally distinctive dissolved organic compounds for the adjacent estuarine waters. Because changes in CDOM optical properties reflect changes in both CDOM amount and chemical structure, the results of this analysis, along with ancillary measurements of DOM molecular-weight distribution and polydispersity, provide useful insights into the composition and quality of the dissolved organic material exported from the marsh and its potential effects on photochemical and biological processes in the adjacent estuarine ecosystem.

Sites and methods

Study site—The Rhode River is a turbid, eutrophic subestuary on the western shore of Chesapeake Bay in Maryland (38.88°N, 76.53°W). The mean tidal amplitude in the subestuary is 0.3 m, but water level is also affected by weather conditions (Jordan et al. 1986). Salinity varies seasonally from 5 to 18 at the mouth of the Rhode River, depending mainly on the flow of the Susquehanna River, and from 0 to 14 at the head, depending mainly on the flow of Muddy Creek, the primary tributary and freshwater source to the subestuary (Gallegos et al. 2005). Muddy Creek is surrounded by a 23-km^2 watershed and consists of 0.23 km^2 of shallow mud flat and creeks bordered by 0.22 km^2 of high-elevation marsh and 0.13 km^2 of low-elevation marsh (Jordan et al. 1986). Our study site (sta. A in Fig. 1) was located at the mouth of a creek (38.8755°N, 76.5463°W) that bisects Kirkpatrick marsh, which is a brackish, high-elevation, tidal marsh south of Muddy Creek (Fig. 1). The marsh is 0.4–0.6 m above mean low water (MLW) and is primarily vegetated by *Spartina patens*, *S. cynosuroides*, *Distichlis spicata*, *Iva frutescens*, and *Scirpus olneyi*. The marsh is fully submerged 2% of the

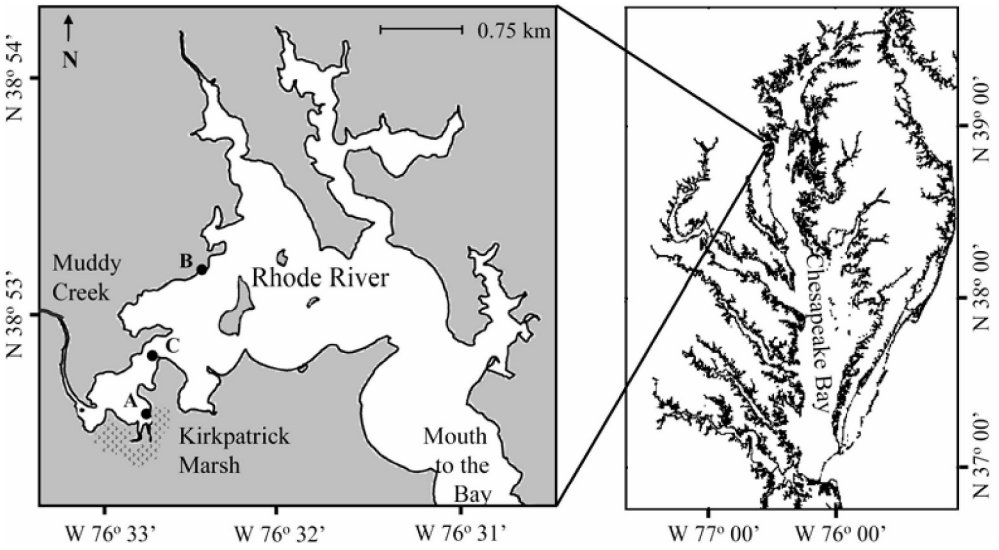

Fig. 1. Left: Map of the Rhode River subestuary showing the Kirkpatrick marsh and the locations of sampling (sta. A, B, and C). Right: Location of the Rhode River subestuary along the western shore of the Chesapeake Bay.

time, and the marsh creek drains an area of ~0.03 km^2 (Jordan and Correll 1991).

Field measurements—To examine the tidal exchange of DOC and CDOM, hourly water samples were collected over 24-h periods from the mouth of the tidal creek (sta. A in Fig. 1) using an ISCO 3700-series compact portable automated sampler. This provided samples of water entering the marsh (i.e., estuarine-dominated samples) and draining the marsh (i.e., marsh-dominated samples) during two adjacent semidiurnal tidal cycles. The ISCO 3700 uses a peristaltic pump for sample collection. Each sampling cycle included a presample and postsample air purge to clear the suction line and minimize cross-contamination. Ice was put in the center of the sampler's base to keep the water samples at low temperature during the duration of sample collection. After a full sample cycle, water samples were filtered immediately through 0.22-μm-pore-diameter polycarbonate membrane filters for optical and compositional analysis of the dissolved material. Measurements performed on two replicate water samples, one left inside the ISCO sampler for 24 h before filtering and the other filtered immediately, showed no significant difference in DOC concentrations [DOC], or CDOM optical properties due to 24-h storage. Filtered water was stored in the dark at 4°C for less than one week. Before optical analysis, the samples were warmed to room temperature.

Measurements of salinity and pH were performed during five of the nine sampled tidal cycles using a YSI 556 multiprobe system. Changes in water depth during the tidal cycle were measured using a bottom-mounted pressure gauge (e.g., Megonigal and Schlesinger 2002) ~1.25 km downstream of the marsh creek (sta. B in Fig. 1; MLW = 1.8 m). Because of the proximity of sta. B (38.8855°N, 76.5416°W) to sta. A (tidal marsh creek) and the 1-h resolution in our water sampling, we assumed that the time of high (or low) tide and the changes in water depth (i.e., tidal range and depth above MLW) at the two sites were essentially the same.

To determine seasonal variability, data were collected during summer (July 2004 and August 2005), when plant biomass in the marsh was peaking, fall (September and October 2004), when vegetation was senescing, and early spring (April 2005), when plant activity was the lowest (Table 1).

CDOM absorption—Measurements of CDOM absorption were performed using a CARY-IV dual-beam spectrophotometer. Due to the high optical thickness of the samples, absorbance measurements were performed using 1-cm path-length, acid-cleaned, quartz cuvettes. Measurements were baseline-corrected using MilliQ water and by running a new blank before each sample. Duplicate measurements were performed for each sample. Measurements covered the spectral range from 290 to 750 nm (1-nm bandwidth and interval). CDOM absorption coefficients were estimated from measured optical densities (OD) after multiplying by 2.303 and dividing by the pathlength l_g (0.01 m for a 1-cm cuvette):

$$a_{\mathrm{CDOM}}(\lambda) = 2.303\frac{\mathrm{OD}}{l_g} = 2.303\frac{\mathrm{OD}}{0.01}(m^{-1}) \qquad (1)$$

Since absorption by CDOM decreases with increasing wavelength in an exponential fashion, the exponential slope, S_{CDOM}, was estimated after applying nonlinear exponential regression to $a_{\mathrm{CDOM}}(\lambda)$ measured in the complete spectral range of the measurements 290–750 nm (Blough and Del Vecchio 2002). R^2 values of the nonlinear exponential fits were in almost all cases >0.99. The average range between duplicate determinations of S_{CDOM} was 0.0001 nm^{-1}. Whereas variability in CDOM absorption reflects changes in both CDOM amount and chemical

Table 1. Dates of water sampling in the Rhode River marsh and tidal range, salinity, dissolved organic carbon concentrations [DOC] (mg L^{-1}), CDOM absorption $a_{CDOM}(440)$ (m^{-1}), CDOM absorption spectral slope S_{CDOM} (nm^{-1}), and synchronous fluorescence SF ($\times 10^5$, arbitrary units) for excitation at 350 nm and emission at 364 nm, measured during the first (A) and second (B) low tide (LT) and high tides (HT) observed (n.d., no data).

Date	Tidal Range (m)	Salinity		[DOC] (mg L^{-1})		$a_{CDOM}(440)$ (m^{-1})		S_{CDOM} (nm^{-1})		SF ($\times 10^5$)	
		LT	HT	LT	HT	LT	HT	LT	HT	LT	HT
20–21 Jul 04, A	0.18	n.d.	n.d.	10.9	5.2	4.77	1.41	0.0143	0.0174	7.2	3.6
20–21 Jul 04, B	0.33	n.d.	n.d.	13.5	6.1	7.01	1.82	0.0143	0.0165	7.2	3.3
16–17 Sep 04, A	0.34	n.d.	n.d.	10.7	5.3	5.03	1.80	0.0152	0.0166	6.1	3.4
16–17 Sep 04, B	0.29	n.d.	n.d.	11.2	5.0	5.80	2.21	0.0151	0.0162	6.9	4.0
21–22 Oct 04	0.34	4.60	5.38	4.7	3.4	2.32	0.89	0.0156	0.0175	3.2	2.2
11–12 Apr 05, A	0.16	2.29	3.07	5.8	4.3	2.85	1.36	0.0152	0.0164	3.6	2.0
11–12 Apr 05, B	0.51	2.33	3.07	7.1	2.9	3.91	0.78	0.0150	0.0176	4.2	2.5
24–25 Aug 05, A	0.41	9.72	10.28	8.0	5.5	5.82	2.19	0.0146	0.0164	6.8	3.4
24–25 Aug 05, B	0.41	10.28	10.38	6.3	4.4	5.82	2.51	0.0152	0.0163	5.4	3.1

structure, variability in the mass-specific CDOM absorption is related only to CDOM composition. Although not all of DOC is colored, CDOM absorption at 440 nm was normalized to DOC concentration, $a^*_{CDOM}(\lambda) = a_{CDOM}(440)/[DOC]$, as a measure of CDOM absorption per unit dissolved organic carbon concentration.

CDOM fluorescence—Measurements of CDOM fluorescence were made on a SPEX Fluoromax-3 spectrofluorometer (Jobin Yvon Horiba). The fluorescence emission measured by the signal-detector, S_c, was referenced to the signal measured by the reference-detector, R_c, in order to monitor and correct for fluctuations in the lamp output, according to manufacturer's protocol. Emission and excitation correction-factor files were applied according to manufacturer instructions to correct for the wavelength dependencies of the optical components of each monochromator and the detectors themselves. Fluorescence spectra were corrected for absorption within the sample (inner-filter effect) according to McKnight et al. (2001) and using the CDOM absorption spectra measured spectrophotometrically. Bandwidths were set to 5 nm for both excitation and emission. A spectrum of MilliQ water was subtracted as a blank to correct for Raman effects.

The synchronous fluorescence (SF) technique was used to investigate variability in composition and optical properties of CDOM in this marsh–estuarine system. An SF spectrum is a subset of the excitation–emission matrix in which excitation and emission are at a constant wavelength offset ($\delta\lambda = \lambda_{em} - \lambda_{exc}$) (Lloyd 1971; Ferrari and Mingazzini 1995). A wavelength offset of $\delta\lambda = 14$ nm was used in our SF measurements (λ_{em} in the range 300–620 nm, 1-nm resolution) based on previous results, which showed that this wavelength offset is optimal for resolving differences in CDOM between sources (Belzile et al. 2002). This wavelength offset is also a good compromise between more structural features and lower signal-to-noise ratios in the SF spectra. The average range between duplicate measurements of SF at excitation 350 nm was 1.6%. In addition, emissions at 470 nm and 520 nm were measured at excitation of 370 nm in order to calculate the fluorescence index (e.g., Cory and McKnight 2005).

Dissolved organic carbon—Samples for DOC analysis were filtered through 0.22-μm filters into cleaned and precombusted (500°C, 5 h) glass vials. To each vial, a few drops of 85% H_3PO_4 was added to decrease the sample pH to <3 and convert all dissolved inorganic carbon (DIC) to CO_2, which was removed by sparging the sample for 10 min with ultrahigh-purity (UHP) He. After removal of DIC, samples were placed in the autosampler of an OI Analytical 1010 TOC (total organic carbon) Analyzer, and DOC was measured by heated persulfate oxidation. Two milliliters of sample were injected into the reaction vessel, and 5 mL of 200 mg L^{-1} persulfate reagent was added. The sample plus reagent was heated to 98°C for 6 min, converting DOC to CO_2. The CO_2 was purged from the sample with UHP He and swept past a nondispersive infrared detector (NDIR) for quantitation. Solutions of potassium hydrogen phthalate standard were used to create a calibration curve over the range of 0 to 833 μmol C L^{-1}. Following the recommendations of McKenna and Doering (1995), enough persulfate was added to the sample so that any halogens present would be oxidized along with DOC. Multiple MilliQ water blanks were run until background counts were low and steady before proceeding with sample analysis. The analytical reproducibility of these measurements was $\sim \pm 3\%$.

DOC fluxes—To quantify the export of DOC from the marsh, we calculated DOC fluxes using our measurements of water depth and [DOC] and estimates of water flow based on a previous study for the same marsh by Jordan and Correll (1991). Jordan and Correll used automated instruments to measure tidal flows (m^3 s^{-1}) at the mouth of the creek over a 3-yr period (1987–1989). Based on their measurements, they estimated the area, A, covered by the water flowing in and out of the marsh (flow per change in depth) as a function of water depth above MLW, $z_{w(>MLW)}$, (their Fig. 3, left panel). We applied this relationship to our hourly ($\Delta t = t_{(i+1)} - t_{(i)} = 1$ h) measurements of $z_{w(>MLW)}$ and water-depth change, Δz_w, during a tidal cycle and estimated hourly DOC fluxes (g s^{-1}) as the product of DOC concentration and flow according to:

$$DOC_{flux} = \overline{[DOC]} \times \Delta z_w / \Delta t \times A(\bar{z}_{w(>MLW)}) \qquad (2)$$

where $\overline{[DOC]}$ is the average [DOC] at $t_{(i)}$ and $t_{(i+1)}$, and $\bar{z}_{w(>MLW)}$ is the average $z_{w(>MLW),}$ at $t_{(i)}$ and $t_{(i+1)}$ at the tidal creek. DOC fluxes during flooding tide ($\Delta z_w > 0$) are shown as positive values in the Results section, while DOC fluxes during ebbing tide ($\Delta z_w < 0$) are shown as negative values. The total DOC discharge from the marsh during ebbing tide, $DOC_{flux,ebb}$, was estimated for each tidal cycle by integrating DOC_{flux} from high to low tide. Similarly, the total flux of DOC entering the marsh during flooding tide, $DOC_{flux,flood}$, was estimated by integrating DOC_{flux} from low to high tide.

Molecular-weight distribution—DOM molecular-weight distribution was measured using size exclusion chromatography (SEC) as reported elsewhere (Maie et al. 2004; Scully et al. 2004). Briefly, the analyses were performed on a Shimadzu (Model LC-10AT) HPLC (high performance liquid chromatography) system fitted with a YMC-Pack Diol-120G size exclusion column (pore size = 12 nm, inner diameter = 8.0 mm, length = 500 mm; YMC). The eluant used was 0.05 M Tris(hydroxymethyl) aminomethane (THAM) adjusted to pH 7.0 with phosphoric acid at a flow rate of 0.7 mL min^{-1}. A UV-Vis detector was used with the absorption set at 280 nm. The injection volume was 150 μL. The void volume (V_0, 14.5 min) and void volume plus inner volume ($V_0 + V_I$, 32.3 min) were determined using Blue Dextran 2000 (Pharmacia) and phenylalanine, respectively. The column was calibrated using Dextran standards of different and known molecular weights (Sigma Chemical). The weight-average molecular weight (M_w) was calculated as follows: $M_w = \Sigma(Ai Mi)/\Sigma Ai$, where Ai and Mi are, respectively, the absorbance in arbitrary units, and the molecular weight was estimated from the calibration curve at elution volume i. DOM polydispersity (d) was calculated as follows: $d = M_w/M_n$, where M_n (number-average molecular weight) was calculated using the equation $M_n = \Sigma Ai/\Sigma(Ai/Mi)$. Determining molecular weight distributions of DOM by SEC-HPLC with UV detection has been commonly reported in the literature (e.g., Her et al. 2003; Maie et al. 2004). However, M_w for DOM components may not be accurate because adequate calibration standards are not readily available, and some DOM components do not have a strong absorbance at 280 nm. For this reason, and because the main objective of this study was to examine relative changes in the average size of DOM during the tidal cycle, M_w is shown here normalized to the values measured at low tide for the marsh-derived DOM (relative units).

Results

Tidal range and salinity—Tidal range during our measurements varied between 0.16 and 0.51 m (Table 1). Both the lowest and highest range occurred during our spring sampling (11–12 April 2005) when the tidal amplitude during two consecutive semidiurnal cycles was considerably different (Fig. 2). Water level above mean low water, $z_{w(>MLW)}$, ranged between –0.01 and 0.14 m at low tide and between 0.27 and 0.65 m at high tide, except during the tidal cycle in October, when the water level was considerably higher than average conditions (Fig. 2). During that sampling date, $z_{w(>MLW)}$ ranged between 0.36 m at low tide and 0.71 m at high tide. Salinity varied widely among sampling dates, with values at high tide ranging between 3.07 (April) and 10.38 (August). However, the variation in salinity, and also in pH (data not shown), was small during individual tidal cycles (in all cases, salinity varied by less than 1 unit; Table 1).

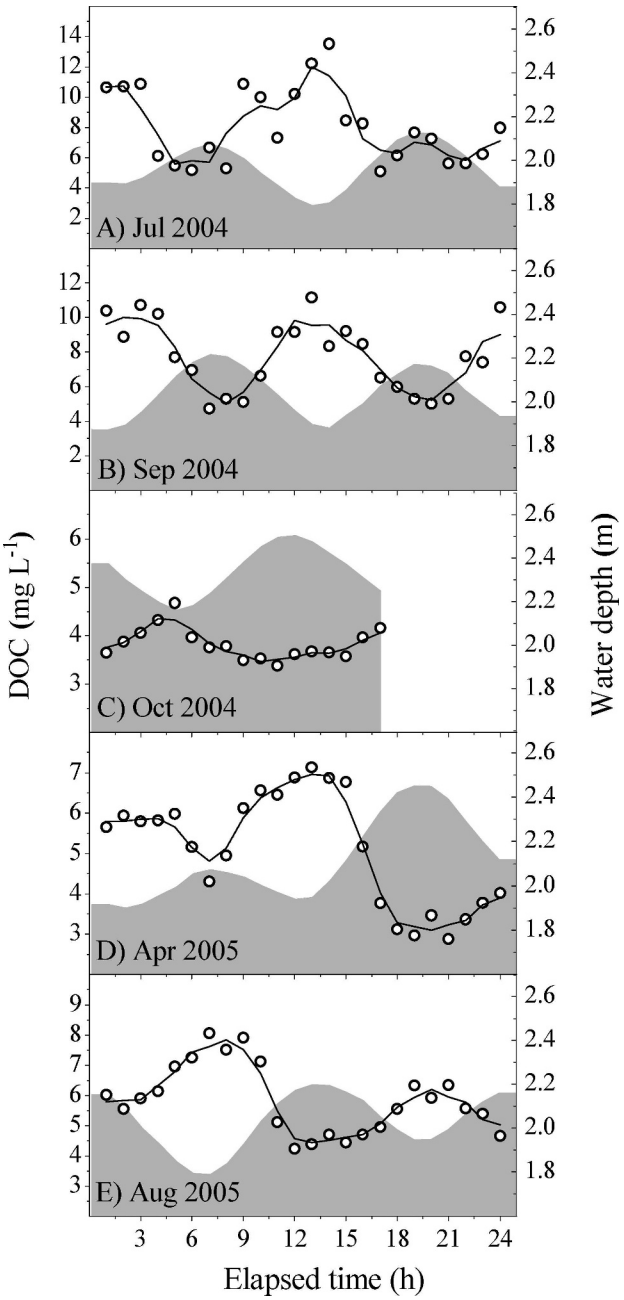

Fig. 2. Tidal exchange of DOC (mg L^{-1}) in the Kirkpatrick marsh during each 24-h period sampled (open circles and smoothed average are shown as a solid line, left axis). During October 2004 (panel C), samples were collected during a 17-h period. Change in water depth (m), as measured at sta. B, is shown in gray (right axis). Elapsed time (h) since beginning of measurements is shown on x-axis.

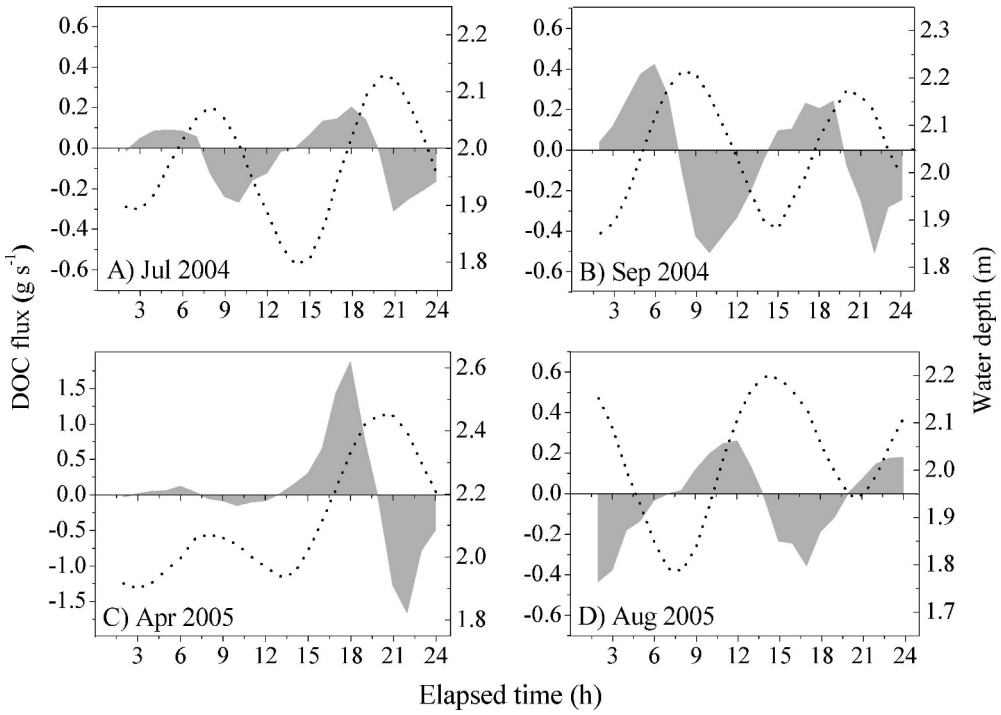

Fig. 3. DOC fluxes (gray area, left axis) estimated at the marsh site during each 24-h period sampled. Change in water depth (m) is shown as dotted line (right axis). Negative fluxes represent DOC export from the marsh to the adjacent tidal creek.

Tidal exchange of DOC—DOC concentrations showed large variation over each tidal cycle and followed a pattern that was very consistent throughout the year (Fig. 2). During each tidal cycle, [DOC] was the lowest at high tide. As water started draining off of the marsh during ebbing tide, DOC gradually increased, reaching maximum concentrations at low tide. [DOC] decreased again as water started flowing into the marsh during the following flooding tide. Water draining from the marsh at low tide was frequently more than twofold enriched in DOC (Table 1). Depending on the season, [DOC] in the estuarine water adjacent to the marsh (high tide data) ranged between 2.9 and 6.1 mg L^{-1}, with an average value of 4.7 mg L^{-1} (standard deviation [SD] = 1.0). We observed the highest DOC levels during the summer and early fall measurements.

DOC fluxes were consistently larger (in absolute value) at ebbing tide compared to flooding tide (Fig. 3). Gross DOC fluxes varied several-fold between cycles as would be expected given the variation in tidal range. However, estimates of the net exchange of DOC at the tidal creek, calculated as the difference between the total DOC export from the marsh and the total DOC import into the marsh during each individual tidal cycle ($|DOC_{flux,ebb}| - |DOC_{flux,flood}|$), indicated a consistent net export of DOC from the marsh to the estuary. Net DOC export was largest during our summer measurements (July 2004). On average, estimated net DOC export was 1.4 kg DOC per tidal cycle. For a drainage area of 0.03 km^2 (Jordan and Correll 1991), this corresponds to 32 g DOC m^{-2} yr^{-1}.

Marsh CDOM optical properties—Absorption and fluorescence analysis revealed some seasonal variation in the optical properties of CDOM in the Rhode River estuarine waters. For the CDOM in the estuarine water flowing into the marsh at high tide, absorption at 440 nm was in the range of 0.78 to 2.51 m^{-1}, and SF magnitude at an emission wavelength of 364 nm (λ_{exc} = 350 nm) varied between 2 and 4 × 10^5 (arbitrary units). Absorption and fluorescence magnitudes were both higher during our summer and early fall measurements (Table 1). S_{CDOM} ranged between 0.0162 and 0.0176 nm^{-1} and did not show any strong seasonal pattern.

The optical properties of CDOM at the tidal marsh creek also varied over short, tidal timescales. The tidal change in CDOM optical properties was consistent and qualitatively very similar for all our sampling dates during seasons of both high and low plant productivity in the marsh. Therefore, data are shown and discussed in detail only for one data set obtained on 16–17 September 2004 (Fig. 4). The two semidiurnal tidal cycles sampled that day were fairly symmetrical. The tidal range (0.34 and 0.29 m) and $z_{w\ (>MLW)}$ at low tide (0.07 and 0.08 m) were close to average conditions for the Rhode River estuarine system. Results for the rest of our sampling dates are summarized in Table 1.

CDOM absorption during the first tidal cycle sampled in September varied by more than a factor of three. The lowest values were observed, throughout the spectrum, at high tide, and the highest values were observed at low tide. Note that only absorption at 440 nm is shown in Fig. 4A

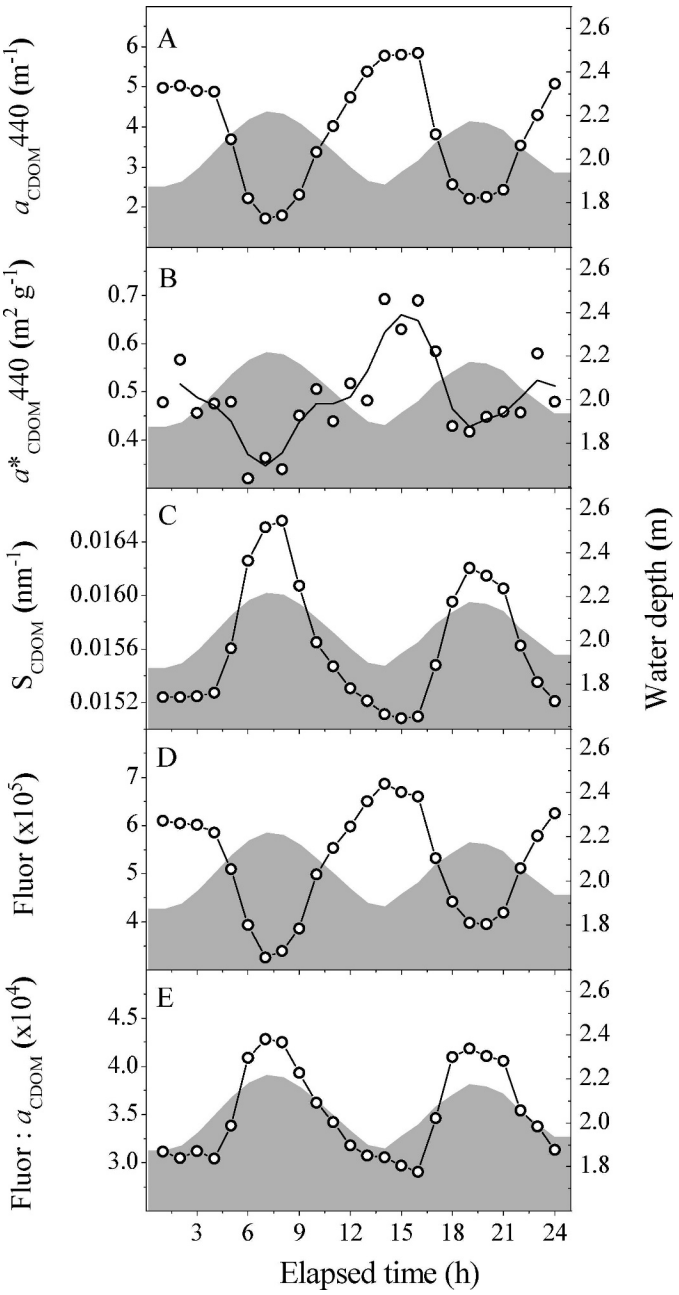

Fig. 4. Tidal cycle variation in CDOM optical properties as a function of elapsed time since beginning of measurements (h) for the tidal cycle sampled on 16–17 September 2004. Change in water depth (m) is shown in all panels (gray area, right axis). Left axis: tidal cycle variation in (A) $a_{CDOM}(440)$ (m^{-1}; solid line with circles), (B) a^*_{CDOM} (440) (m^2 g^{-1}; shown as circles; smoothed average is shown as a solid line), (C) S_{CDOM} (nm^{-1}; solid line with circles), (D) synchronous fluorescence (arbitrary units, excitation: 350 nm, emission: 364 nm) (solid line with circles), and (E) synchronous fluorescence (i.e., panel D) normalized to $a_{CDOM}(350)$ (relative yield; solid line with circles).

and Table 1 because this is often chosen as the reference wavelength for CDOM absorption (e.g., Carder et al. 1989; Gallegos et al. 2005). About half of the measured range in $a_{CDOM}(440)$ was due to variation in [DOC] (Fig. 2), while the other half was due to a parallel variation in DOC-specific absorption. We observed a minimum $a^*_{CDOM}(440)$ of 0.33 m^2 g^{-1} close to high tide, a gradual increase during ebbing tide, and a maximum $a^*_{CDOM}(440)$ of 0.69 m^2 g^{-1} at the following low tide (Fig. 4B). Moreover, CDOM draining off of the marsh was characterized by significantly lower absorption spectral slope, S_{CDOM}, relative to CDOM in the adjacent estuarine waters (Fig. 4C). S_{CDOM} in the water flowing out of the marsh was 0.0152 nm^{-1}, it steadily increased with flooding tide to a maximum value of 0.0166 nm^{-1} at high tide, and it decreased again to 0.0151 nm^{-1} at the following low tide. During our sampling dates throughout the year, average $a_{CDOM}(440)$ and S_{CDOM} were 4.81 m^{-1} (SD = 1.53) and 0.0149 nm^{-1} (SD = 0.0004), respectively, at low tide, compared to 1.66 m^{-1} (SD = 0.60) and 0.0168 nm^{-1} (SD = 0.0006) at high tide.

In addition to having high absorbance, CDOM draining off of the marsh at low tide had high fluorescence relative to CDOM flowing into the marsh at high tide. Diurnal variation in the CDOM synchronous fluorescence paralleled variations in [DOC], $a_{CDOM,}$ and a^*_{CDOM}; the lowest fluorescence was measured in the CDOM collected at high tide, and the highest fluorescence was measured in the CDOM collected at low tide (only diurnal variation in SF for excitation at 350 and emission at 364 nm is shown in Fig. 4D and Table 1). SF at excitation 350 nm was less variable than $a_{CDOM}(350)$. The ratio of SF to absorption, used here as a measure of the fluorescence yield, was lower for marsh-derived CDOM compared to estuarine CDOM (Fig. 4E). Maximum SF was measured at an emission wavelength of ~365 nm throughout the tidal cycle (Fig. 5). However, CDOM exported from the marsh had stronger SF at wavelengths longer than 400 nm and a more pronounced shoulder in the spectral region around 490 nm. We estimated the ratio $SF_{em490}:SF_{em365}$ as a measure of the differences in the spectral shape of SF during the tidal cycle. This ratio was considerably higher at low tide (Fig. 5). The ratio of fluorescence emission intensity at wavelength 470 nm to that at 520 nm, obtained with an excitation at 370 nm (fluorescence index, FI), has been used in previous studies as a simple index to distinguish sources of isolated aquatic fulvic acids (e.g., Cory and McKnight 2005). For our measurements in the marsh creek, this fluorescence index was relatively smaller for CDOM exiting the marsh compared to CDOM entering the marsh, but in all cases, it was less than 1.4.

Marsh DOM molecular-weight distribution—DOM exported from the Rhode River marshes at low tide had considerably higher average molecular weight, M_w, and polydispersity, d, compared to DOM imported to the marshes at high tide (Fig. 6). The measured SEC elution curves for marsh-derived DOM showed three peaks, one at an elution time of 22.2 min with a shoulder at 23 min, one at 24.8 min, and one at 28.8 min (Fig. 7). These peaks and shoulders were observed in all DOM samples collected over the tidal cycle. However, the larger M_w fraction of the first peak gradually decreased as water from the adjacent estuary started flowing into the marsh at flooding tide (data not shown) and was absent (i.e., loss of left shoulder)

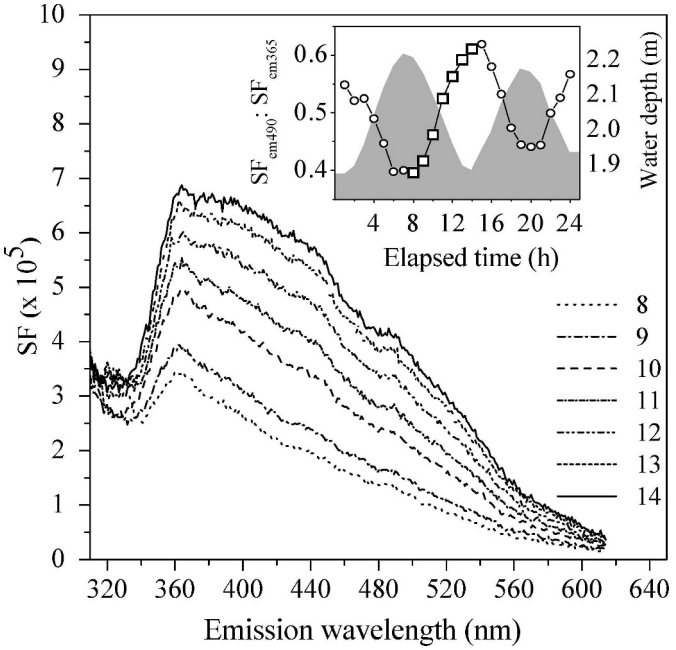

Fig. 5. Synchronous fluorescence (SF) spectra of DOM collected from the tidal marsh creek during the transition from high tide to low tide, which correspond to elapsed times of 8 h and 14 h, respectively, from the start of sampling on 16–17 September 2004. Inset: Tidal cycle variation in $SF_{em490}:SF_{em365}$ (solid line with circles) and water depth (gray area) as a function of elapsed time (h).The transition from high tide (8 h) to low tide (14 h) is shown as squares in the inset. The average range between duplicate measurements of the ratio $SF_{em490}:SF_{em365}$ was 0.01.

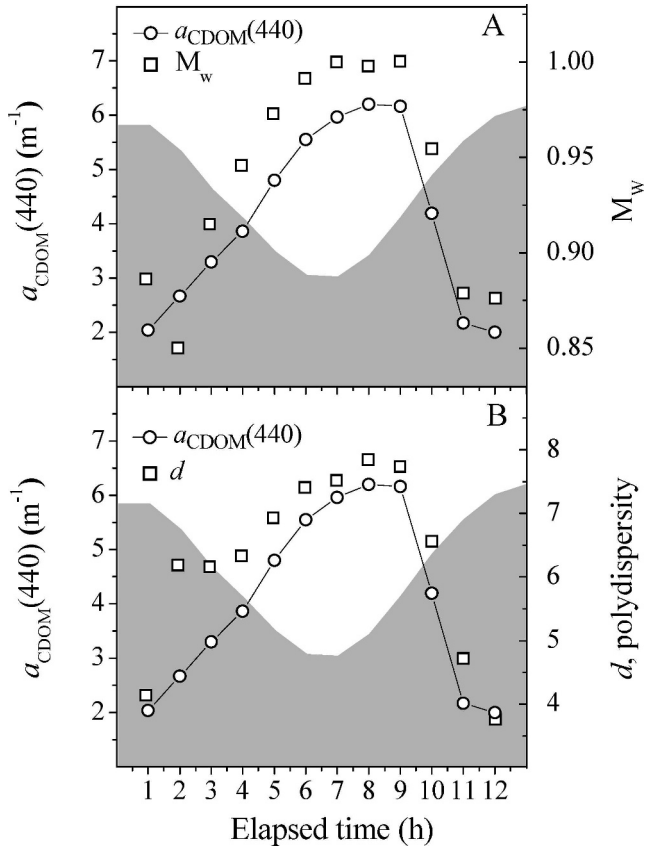

Fig. 6. (A) Change in $a_{CDOM}(440)$ (m^{-1}) and weight-average molecular weight, M_w (relative units, M_w is normalized to the values measured at low tide for the marsh-derived DOM). (B) Change in $a_{CDOM}(440)$ (m^{-1}) and polydispersity, d, during one tidal cycle in the Kirkpatrick marsh (24 August 2005). Change in water depth as a function of elapsed time since beginning of measurements is shown as gray area.

in the elution curves of DOM collected at high tide (Fig. 7). Moreover, for DOM at high tide, the elution peaks with longer retention times (i.e., peaks at 24.8 and 28.8 min), which correspond to smaller-molecular-size region, were higher in both absolute and relative (DOC-specific) abundance. The twofold increase in polydispersity values during ebbing tide (Fig. 6B) reflects the larger range in molecular weight in the first elution peak of the marsh-derived CDOM. Measured diurnal variations in M_w and d were strongly correlated with observed variation in CDOM absorption over the tidal cycle. Coefficients of determination (R^2) were 0.93 and 0.89 between M_w and $a_{CDOM}(440)$ and between d and $a_{CDOM}(440)$, respectively.

Discussion

Tidal marshes along coastal margins have been previously shown to be important sources of DOC, contributing to the carbon budgets of nearshore waters (e.g., Nixon 1980; Moran and Hodson 1994; Peterson et al. 1994). In agreement with these studies, we found that the Kirkpatrick tidal marshes are, indeed, an important source of DOC for the Rhode River subestuary throughout the year. Analysis of a 2-yr data set (2004–2005; T. E. Jordan unpubl. data) collected from sta. C in the estuarine waters adjacent to the Kirkpatrick marsh (38.881°N, 76.545°W; Fig. 1) suggests that average [DOC] in these estuarine

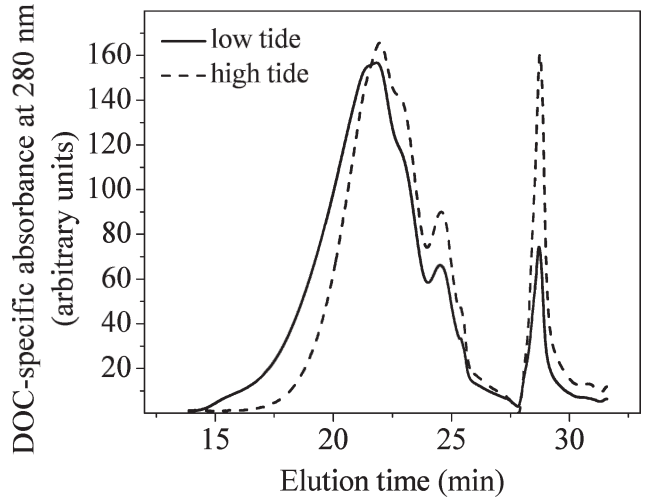

Fig. 7. Elution curves of DOM collected from the Kirkpatrick marsh at low tide and at high tide (24 August 2005). The elution curve was recorded by measuring the absorbance of the eluent at 280 nm, and results were normalized to [DOC] (arbitrary units).

waters is about 4 mg L^{-1} (SD = 1.44). Relatively low DOC concentrations typically occur from mid-fall to late spring, consistent with long-term monitored biological activity in these waters (Gallegos et al. 2005). Both our measured DOC concentrations in the water imported into the marsh during flooding tide and their seasonal variability agreed well with these previous observations. In addition, our measurements during ebbing tide revealed that DOC levels at the marsh creek consistently increased, frequently by more than a factor of two, as dissolved material drained from the marsh (Fig. 2). Export of DOC from the marsh to the estuary occurred during seasons of both high and low biological activity. Although based on a limited number of sampled tidal cycles, our estimate of average net DOC export was consistent with the value of 43 g DOC m^{-2} yr^{-1} estimated by Jordan et al. (1983), who composited flood and ebb water DOM samples collected from the same marsh–estuarine system during 11 tidal cycles in 1980–1981. The small change in salinity (less than 1) during each sampled tidal cycle indicates that the effect of freshwater inputs on DOC exchanges by the marsh was relatively small during our measurements.

Because a large fraction of DOC is optically active, the observed marsh tidal discharges would be expected to have a large influence, not only on estuarine carbon cycling, but also on the estuary's water optical properties and CDOM dynamics. Indeed, our optical analysis showed that water flowing out of the marsh, in addition to being a source of DOC for the estuary, is also an important source of colored dissolved compounds with distinctive optical characteristics. DOM in the Rhode River is mainly derived from the local watershed and wetlands of Muddy Creek, as well as phytoplankton excretion and lysis, and benthic decomposition of settled phytoplankton and organic matter (Gallegos et al. 2005). Thus, CDOM present in these estuarine waters (herein referred to as ''estuarine-dominated'' CDOM) typically has high absorption. Measurements of CDOM absorption at sta. C during a 3-yr period covering the months of April to October (1999–2001; C. L. Gallegos unpubl. data) showed that average $a_{CDOM}(440)$ in the water adjacent to the Kirkpatrick marsh was about 0.81 m^{-1} (SD = 0.3), with an average S_{CDOM} of 0.0177 nm^{-1} (SD = 0.0012). Higher values of CDOM absorption typically occur during summer (Gallegos et al. 2005). These results are consistent with the a_{CDOM} and S_{CDOM} values that we measured in the water flowing into the marsh. Our measurements further revealed that dissolved material in the DOC-enriched water draining from the marshes consistently had two to five times higher absorption, as well as higher fluorescence, than estuarine-dominated CDOM (Table 1; Figs. 4, 5). These observations suggest that, throughout the year, marsh export of colored DOM drives substantial variation in underwater light availability over short, tidal timescales, significantly affecting CDOM dynamics and, thus, estuarine optics, color, and photochemistry.

The importance of salt marshes as contributors to the CDOM budget in estuarine waters was previously studied by Gardner et al. (2005) for the tidal estuary of Neponset River in Dorchester Bay, Massachusetts. Using changes in CDOM fluorescence as an indicator of changes in CDOM absorption and concentration, Gardner et al. concluded that degradation of organic matter derived from a mid-estuary, *Spartina*-dominated, salt marsh was an important seasonal source of CDOM for the estuarine system. However, fluorescence quantum yield and mass-specific absorption were assumed to be constant along the estuarine gradient. In comparing flood tides with ebb tides for a southern California salt marsh system, C. Clark (pers. comm.) found, in agreement with our results, that CDOM absorption magnitude was about two to three times higher for ebb tides than for flood tides. However, their measurements showed that there was no significant difference in the CDOM absorption spectral shape, S_{CDOM}, between the material entering and leaving the sloughs, indicating a single source of CDOM. In contrast, the results of both our absorption and fluorescence analyses suggest that the Kirkpatrick marshes are a source of chemically distinctive dissolved organic compounds.

Although changes in CDOM fluorescence and absorption magnitude are associated with changes in both the composition and concentration of dissolved organic compounds, variability in DOC-specific absorption, S_{CDOM}, fluorescence spectral shape, and fluorescence per unit absorbance reflects changes only in the composition and chemical structure of CDOM (e.g., Stewart and Wetzel 1980; Blough and Green 1995; McKnight et al. 2001). Our estimates of the fluorescence index, FI, for estuarine-dominated dissolved material were consistent with the predominantly terrestrial, versus planktonic, source of CDOM in the Rhode River estuarine system. Relative to this estuarine-dominated CDOM, dissolved material draining off of the Kirkpatrick marshes was consistently characterized by (1) two to four times greater DOC-specific absorption, (2) considerably lower S_{CDOM}, (3) stronger fluorescence at wavelengths longer than 400 nm, (4) lower FI, and (5) lower fluorescence per unit absorbance. As discussed below, all these optical characteristics are indicative of aromatic-rich, less-degraded, high-molecular-weight dissolved organic material, most probably derived from marsh plants and soil leachates.

Molecular weight and the aromatic content of humic substances are ecologically important parameters for understanding humic substance mobility, interactions with nutrients and pollutants, and microbial metabolism in aquatic ecosystems (Chin et al. 1994). DOM susceptibility to microbial degradation, photoreactivity, and optical signature have been shown to vary widely among different molecular-weight fractions (e.g., Amon and Benner 1996; Belzile and Guo 2006; Lou and Xie 2006). Previous studies have suggested that, for humic substances, DOC-specific CDOM absorption typically increases while S_{CDOM} decreases (CDOM absorption at the longer wavelengths increases) with increasing molecular weight and increasing aromaticity (e.g., Blough and Green 1995; Del Vecchio and Blough 2004). Chin et al. (1994) reported an increase in CDOM molar absorptivity at 280 nm with molecular weight and aromatic content. As mentioned in Belzile and Guo (2006), low S_{CDOM} is typical of high-molecular-weight and less-altered CDOM, while a high value is indicative of

low-molecular-weight, highly degraded CDOM (Markager and Vincent 2000; Twardowski et al. 2004).

The ratio of fluorescence to absorption, which we showed to be about 35% lower in the marsh-exported CDOM (Fig. 4B), was first proposed by Stewart and Wetzel (1980) as a tracer of DOM molecular weight in aquatic systems. In their study, naturally occurring dissolved humic materials from a freshwater lake environment were fractionated according to molecular weight. Components of higher molecular weight (>3,500 Daltons) absorbed strongly at 250 nm but fluoresced relatively weakly, while humic fractions of lower molecular weight had larger fluorescence per unit absorbance. Stewart and Wetzel (1981) suggested that the decrease in the fluorescence yield in larger-molecular-weight DOM might be a result of losses in fluorescence emission due to increased levels of self-quenching and internal conversion (Schenk 1973), since larger, more complex DOM molecules have far more energy states than their smaller counterparts. A more recent study by Belzile and Guo (2006), where—similar to our study—fluorescence intensity measurements were corrected for the inner-filter effect (McKnight et al. 2001), showed that high-molecular-weight DOM is indeed characterized by lower fluorescence per unit absorbance compared to low-molecular-weight DOM. Moreover, using SF analysis ($\delta\lambda$ = 14 nm, as in our study), Belzile et al. (2002) showed that plant- and soil-derived fulvic acids of relatively high-molecular-weight and aromatic-carbon content typically have stronger SF peaks at wavelengths longer than 400 nm relative to microbially derived fulvic acids of lower-molecular-weight and aromatic-carbon content. Consistent with expectations based on the rest of our optical analysis, marsh-derived CDOM was characterized by a relatively strong SF signal at wavelengths longer than 400 nm.

The results on the molecular-weight distribution support our inferences about DOM molecular structure drawn from CDOM optical analysis. Humic acids and soil humic substances generally have higher heterogeneities, as represented by higher polydispersity, than fulvic acids and aquatic humic substances (e.g., O'Loughlin and Chin 2001; Perminova et al. 2003). In the Kirkpatrick marsh system, marsh-derived CDOM was associated with higher average M_w distributions, while CDOM in the adjacent waters was characterized by higher absolute and relative abundance of low-molecular-weight material and reduced polydispersity. It is highly unlikely that such variations between high and low tide could be caused by salinity changes, which can induce analytical artifacts in the SEC analysis, because salinity variations were minimal.

The observed differences in optical properties, molecular weight, and polydispersity between CDOM in the water flowing into and out of the marsh may be due to differences in the source of DOM, where marsh plants and soil leachates are the main source of DOM at ebbing tide, and DOM at flooding tide is a mixture of predominantly terrestrial, watershed-derived, material with some phytoplankton-derived DOM. Moreover, photochemically induced transformations and microbial processing of DOM could also affect CDOM optical properties and molecular weight in the tidal creek. The size reactivity continuum model (Amon and Benner 1996) suggests that, during decomposition, organic matter continuously becomes less bioreactive and smaller in physical size. Microbial metabolism has been shown to modify DOM to lower-molecular-weight molecules (e.g., Kim et al. 2006), while photochemical breakdown of high-molecular-weight DOM during solar exposure generates a variety of photoproducts, including lower-molecular-weight, labile carbonyl compounds (e.g., Kieber et al. 1990; Moran and Zepp 1997; Scully et al. 2004). Opsahl and Benner (1998) showed that extensive photochemical oxidation of lignin macromolecules characteristic of riverine DOM resulted in a major shift in dissolved lignin size distribution and an absolute increase in low-molecular-weight (<1,000 Daltons) lignin concentration. Lou and Xie (2006) found that sunlight-induced photochemical processes significantly reduced both the average molecular size and polydispersity of DOM from different soil and aquatic sources.

Rates of photochemical reactions are expected to be relatively high at interfaces, like tidal marshes, where large concentrations of unexposed DOC are exported from shaded environments to unshaded estuarine waters (Vahatalo and Wetzel 2004). Indeed, Tzortziou et al. (2007) recently demonstrated that CDOM exported from the Kirkpatrick marshes of the Rhode River is strongly photoreactive and, thus, strongly susceptible to photochemical and subsequent microbial degradation. Therefore, photochemical and/or microbial processing of previously exported, high-molecular-weight, marsh-derived DOM, mixed with autochthonous DOM in the estuary, most likely contributes to the increased relative abundance of less-complex, lower-molecular-weight DOM observed in the waters adjacent to the marsh. More studies of CDOM along transects from the marsh to the mouth of the subestuary are necessary in order to determine the degree of transformation and fate of marsh-exported DOM during transport to the Chesapeake Bay.

References

Alberts, J. J., M. Takacs, and J. Schalles. 2004. Ultraviolet-visible and fluorescence spectral evidence of natural organic matter (NOM) changes along an estuarine salinity gradient. Estuaries **27:** 296–310.

Amon, R. M. W., and R. Benner. 1996. Bacterial utilization of different size classes of dissolved organic matter. Limnol. Oceanogr. **41:** 41–51.

Belzile, C., J. A. E. Gibson, and W. F. Vincent. 2002. Colored dissolved organic matter and dissolved organic carbon exclusion from lake ice: Implications for irradiance transmission and carbon cycling. Limnol. Oceanogr. **47:** 1283–1293.

———, and L. D. Guo. 2006. Optical properties of low molecular weight and colloidal organic matter: Application of the ultrafiltration permeation model to DOM absorption and fluorescence. Mar. Chem. **98:** 183–196.

Blough, N. V., and R. Del Vecchio. 2002. Chromophoric DOM in the coastal environment, p. 509–546. *In* D. A. Hansell and C. A. Carlson [eds.], Biogeochemistry of marine dissolved organic matter. Academic Press.

———, AND S. A. GREEN. 1995. Spectroscopic characterization and remote sensing of nonliving organic matter, p. 23–45. *In* R. G. Zepp and C. Sonntag [eds.], Role of nonliving organic matter in the Earth's carbon cycle. John Wiley & Sons.

BRICAUD, A., A. MOREL, AND L. PRIEUR. 1981. Absorption by dissolved organic matter of the sea (yellow substance) in the UV and visible domains. Limnol. Oceanogr. **26:** 43–53.

CARDER, K. L., R. G. STEWARD, G. R. HARVEY, AND P. B. ORTNER. 1989. Marine humic and fulvic-acids—their effects on remote-sensing of ocean chlorophyll. Limnol. Oceanogr. **34:** 68–81.

CHIN, Y. P., G. AIKEN, AND E. O'LOUGHLIN. 1994. Molecular-weight, polydispersity, and spectroscopic properties of aquatic humic substances. Environ. Sci. Tech. **28:** 1853–1858.

CORY, R. M., AND D. M. MCKNIGHT. 2005. Fluorescence spectroscopy reveals ubiquitous presence of oxidized and reduced quinones in dissolved organic matter. Environ. Sci. Tech. **39:** 8142–8149.

DEL VECCHIO, R., AND N. V. BLOUGH. 2004. On the origin of the optical properties of humic substances. Environ. Sci. Tech. **38:** 3885–3891.

FERRARI, G. M., AND M. MINGAZZINI. 1995. Synchronous fluorescence spectra of dissolved organic matter (DOM) of algal origin in marine coastal waters. Mar. Ecol. Prog. Ser. **125:** 305–315.

GALLEGOS, C. L., T. E. JORDAN, A. H. HINES, AND D. E. WELLER. 2005. Temporal variability of optical properties in a shallow, eutrophic estuary: Seasonal and interannual variability. Estuar. Coast. Shelf Sci. **64:** 156–170.

GARDNER, G. B., R. F. CHEN, AND A. BERRY. 2005. High-resolution measurements of chromophoric dissolved organic matter (CDOM) in the Neponset River Estuary, Boston Harbor, MA. Mar. Chem. **96:** 137–154.

HEDGES, J. I. 1992. Global biogeochemical cycles—progress and problems. Mar. Chem. **39:** 67–93.

HER, N., G. AMY, D. MCKNIGHT, J. SOHN, AND Y. M. YOON. 2003. Characterization of DOM as a function of MW by fluorescence EEM and HPLC-SEC using UVA, DOC, and fluorescence detection. Water Res. **37:** 4295–4303.

JAFFÉ, R., J. N. BOYER, X. LU, N. MAIE, C. YANG, N. SCULLY, AND S. MOCK. 2004. Sources characterization of dissolved organic matter in a mangrove-dominated estuary by fluorescence analysis. Mar. Chem. **84:** 195–210.

JORDAN, T. E., AND D. L. CORRELL. 1991. Continuous automated sampling of tidal exchanges of nutrients by brackish marshes. Estuar. Coast. Shelf Sci. **32:** 527–545.

———, ———, AND D. F. WHIGHAM. 1983. Nutrient flux in the Rhode River—tidal exchange of nutrients by brackish marshes. Estuar. Coast. Shelf Sci. **17:** 651–667.

———, J. W. PIERCE, AND D. L. CORRELL. 1986. Flux of particulate matter in the tidal marshes and subtidal shallows of the Rhode River Estuary. Estuaries **9:** 310–319.

KIEBER, R. J., X. L. ZHOU, AND K. MOPPER. 1990. Formation of carbonyl-compounds from UV-induced photodegradation of humic substances in natural waters—fate of riverine carbon in the sea. Limnol. Oceanogr. **35:** 1503–1515.

KIM, S., L. A. KAPLAN, AND P. G. HATCHER. 2006. Biodegradable dissolved organic matter in a temperate and a tropical stream determined from ultra-high resolution mass spectrometry. Limnol. Oceanogr. **51:** 1054–1063.

LLOYD, J. B. F. 1971. Synchronized excitation of fluorescence emission spectra. Nat. Phys. Sci. **231:** 64–65.

LOU, T., AND H. X. XIE. 2006. Photochemical alteration of the molecular weight of dissolved organic matter. Chemosphere **65:** 2333–2342.

LU, X. Q., N. MAIE, J. V. HANNA, D. CHILDERS, AND R. JAFFÉ. 2003. Molecular characterization of dissolved organic matter in freshwater wetlands of the Florida Everglades. Water Res. **37:** 2599–2606.

MAIE, N., J. N. BOYER, C. Y. YANG, AND R. JAFFÉ. 2006. Spatial, geomorphological, and seasonal variability of CDOM in estuaries of the Florida Coastal Everglades. Hydrobiologia **569:** 135–150.

———, A. WATANABE, AND M. KIMURA. 2004. Chemical characteristics and potential source of fulvic acids leached from the plow layer of paddy soil. Geoderma **120:** 309–323.

MARKAGER, S., AND W. F. VINCENT. 2000. Spectral light attenuation and the absorption of UV and blue light in natural waters. Limnol. Oceanogr. **45:** 642–650.

MCKENNA, J. H., AND P. H. DOERING. 1995. Measurement of dissolved organic carbon by wet chemical oxidation with persulfate—influence of chloride concentration and reagent volume. Mar. Chem. **48:** 109–114.

MCKNIGHT, D. M., E. W. BOYER, P. K. WESTERHOFF, P. T. DORAN, T. KULBE, AND D. T. ANDERSEN. 2001. Spectrofluorometric characterization of dissolved organic matter for indication of precursor organic material and aromaticity. Limnol. Oceanogr. **46:** 38–48.

MEGONIGAL, J. P., AND W. H. SCHLESINGER. 2002. Methane-limited methanotrophy in tidal freshwater swamps. Global Biogeochem. Cy. **16:** 1088–1098.

MILLER, W. L., M. A. MORAN, W. M. SHELDON, R. G. ZEPP, AND S. OPSAHL. 2002. Determination of apparent quantum yield spectra for the formation of biologically labile photoproducts. Limnol. Oceanogr. **47:** 343–352.

MORAN, M. A., AND R. E. HODSON. 1994. Dissolved humic substances of vascular plant origin in a coastal marine environment. Limnol. Oceanogr. **39:** 762–771.

———, R. J. WICKS, AND R. E. HODSON. 1991. Export of dissolved organic matter from a mangrove swamp ecosystem—evidence from natural fluorescence, dissolved lignin phenols, and bacterial secondary production. Mar. Ecol. Prog. Ser. **76:** 175–184.

———, AND R. G. ZEPP. 1997. Role of photoreactions in the formation of biologically labile compounds from dissolved organic matter. Limnol. Oceanogr. **42:** 1307–1316.

NIXON, S. W. 1980. Between coastal marshes and coastal waters—a review of twenty years of speculation and research on the role of salt marshes in estuarine productivity and water chemistry, p. 438–525. *In* P. Hamilton and K. MacDonald [eds.], Estuarine and wetland processes. Plenum.

O'LOUGHLIN, E., AND Y. P. CHIN. 2001. Effect of detector wavelength on the determination of the molecular weight of humic substances by high-pressure size exclusion chromatography. Water Res. **35:** 333–338.

OPSAHL, S., AND R. BENNER. 1997. Distribution and cycling of terrigenous dissolved organic matter in the ocean. Nature **386:** 480–482.

———, AND ———. 1998. Photochemical reactivity of dissolved lignin in river and ocean waters. Limnol. Oceanogr. **43:** 1297–1304.

PERMINOVA, I. V., F. H. FRIMMEL, A. V. KUDRYAVTSEV, N. A. KULIKOVA, G. ABBT-BRAUN, S. HESSE, AND V. S. PETROSYAN. 2003. Molecular weight characteristics of humic substances from different environments as determined by size exclusion chromatography and their statistical evaluation. Environ. Sci. Tech. **37:** 2477–2485.

PETERSON, B., B. FRY, M. HULLAR, S. SAUPE, AND R. WRIGHT. 1994. The distribution and stable carbon isotopic composition of dissolved organic carbon in estuaries. Estuaries **17:** 111–121.

Pienitz, R., and W. F. Vincent. 2000. Effect of climate change relative to ozone depletion on UV exposure in subarctic lakes. Nature **404:** 484–487.

Schenk, G. H. 1973. Absorption of light and ultraviolet radiation: Fluorescence and phosphorescence emission. Allyn and Bacon.

Scully, N. M., N. Maie, S. K. Dailey, J. N. Boyer, R. D. Jones, and R. Jaffé. 2004. Early diagenesis of plant-derived dissolved organic matter along a wetland, mangrove, estuary ecotone. Limnol. Oceanogr. **49:** 1667–1678.

Sholkovitz, E. R. 1976. Flocculation of dissolved organic and inorganic matter during mixing of river water and seawater. Geochim. Cosmochim. Ac. **40:** 831–845.

Stewart, A. J., and R. G. Wetzel. 1980. Fluorescence : absorbance ratios—a molecular-weight tracer of dissolved organic matter. Limnol. Oceanogr. **25:** 559–564.

———, and ———. 1981. Asymmetrical relationships between absorbance, fluorescence, and dissolved organic carbon. Limnol. Oceanogr. **26:** 590–597.

Teal, J. M. 1962. Energy-flow in salt-marsh ecosystem of Georgia. Ecology **43:** 614–624.

Twardowski, M. S., E. Boss, J. M. Sullivan, and P. L. Donaghay. 2004. Modeling the spectral shape of absorption by chromophoric dissolved organic matter. Mar. Chem. **89:** 68–88.

Tzortziou, M., C. L. Osburn, and P. J. Neale. 2007. Photobleaching of dissolved organic material from a tidal marsh-estuarine system of the Chesapeake Bay. Photochem. Photobiol. **83:** 782–792.

Vahatalo, A. V., and R. G. Wetzel. 2004. Photochemical and microbial decomposition of chromophoric dissolved organic matter during long (months-years) exposures. Mar. Chem. **89:** 313–326.

Vodacek, A., N. V. Blough, M. D. Degrandpre, E. T. Peltzer, and R. K. Nelson. 1997. Seasonal variation of CDOM and DOC in the Middle Atlantic Bight: Terrestrial inputs and photooxidation. Limnol. Oceanogr. **42:** 674–686.

Received: 23 January 2007
Accepted: 3 July 2007
Amended: 24 August 2007